ELSEVIER

Chemical Engineering Journal 117 (2006) 223–229

Chemical Engineering Journal

www.elsevier.com/locate/cej

Influence of magnetic field on the fluidization characteristics of circulating fluidized bed

S.K. Dahikar*, R.L. Sonolikar

Laxminarayan Institute of Technology, Nagpur University 440033, Maharashtra, India

Received 31 August 2005; received in revised form 5 January 2006; accepted 10 January 2006

Abstract

This work concerns with the evaluation of a scaled 'magnetically assisted circulating fluidized bed', with a circular cross-section. Flow behavior and solids distributions were determined in a riser (0.032 m i.d. × 1.5 m height) of magnetite particles ($d_p = 425\ \mu m$, $\Phi = 0.86$, $\rho_s = 4500\ kg\ m^{-3}$), in the experimental range ($U_g = 4.2–5.3\ m\ s^{-1}$; $G_s = 30.1–40.3\ kg\ m^{-2}\ s^{-1}$), which covered the fast fluidization flow regime. A shutter arrangement was used to measure the solids circulation rate. The riser is equipped with a pressure tapping at an interval of 0.3 m to detect the axial pressure profile, which helps in calculating the apparent solids holdup in that section. The plots conditions were distinguished by variations of parameters (net solids circulation rate, flow velocity, magnetic field intensity) at various heights along the riser for presence and absence of magnetic field. It is predictable, that the magnetic field has a significant influence on fluidization phenomenon along the whole riser, especially for the dilute section. It appears that, for applied magnetic field, the solids holdup begins to increase, this most likely indicates the starts of a 'transition' towards much 'denser' suspension.

Keywords: Magnetically assisted circulating fluidized bed; Gas–solids flow dynamics; Solids distributions; Hydrodynamics

1. Introduction

Gas–solid reactions occur in a wide range of chemical processes, including coal combustion, fluid catalytic cracking (FCC), fluid hydroforming, the Synthol FischerTropsch synthesis, and the production of maleic anhydride, alkylate and high-purity alumina. The two reactor configurations that are often employed for such reactions are the bubbling fluidized bed and the circulating fluidized bed (CFB). Unlike the bubbling bed, which operates at a relatively low velocity with minimal particle carryover, the CFB unit runs at a velocity high enough to ensure that both the gas and solid phase exit from the top of the reactor. After separation from the gas via a cyclone, the particles are returned to the riser reactor section and thus are continually circulated throughout the CFB reactor. The benefits of the CFB configuration over the bubbling bed include greater contacting between the two phases, higher throughput, and continuous catalyst regeneration if necessary.

Fluid catalytic cracking (FCC) is a trillion dollar worldwide industrial operation that converts heavy hydrocarbons (petroleum) to lower molecular weight products, such as gasoline [1,2]. The development of very active catalysts allowed the cracking to be completed in short-contact-time riser (vertical pipe) reactors. Hence, the older bubbling-bed reactors were replaced with risers. However, it was only a decade ago that the oil industry using gamma-ray techniques [3] learned that their large-diameter risers operate in the core-annular flow regime: the core is very dilute. The core-annular structure leads to two main problems: (1) inefficient gas–solids contact and (2) back mixing due to nonuniform radial distributions [4]. Therdthianwong and Gidaspow [5] reported that the absorption of sulphur dioxide by 210 μm calcined dolomite particle in a riser is much smaller in the dilute core compared to the absorption in the dense core. This unfavorable radial volume fraction distribution of solids in the riser has led to consideration of new schemes of contacting for a refinery of the 21st century.

Here we are mainly concerned with the application of magnetic field to a CFB riser. A conventional CFB with the magnetic field will have a change over due to interparticle attraction [6–8]. In a fast-fluidized bed in which the bottom zone has dense structure and upper dilute region with core-annulus model will

* Corresponding author. Tel.: +91 712 5661736; fax: +91 712 2531659.
E-mail address: skdahikar@yahoo.com (S.K. Dahikar).

1385-8947/$ – see front matter © 2006 Elsevier B.V. All rights reserved.
doi:10.1016/j.cej.2006.01.002

Nomenclature

d_p	particle diameter (μm)
G_s	solid circulation rate (kg m^{-2} s^{-1})
H	magnetic field intensity (A m^{-1})
U_g	superficial gas velocity (m s^{-1})
U_{mf}	minimum fluidization velocity (m s^{-1})
z	axial height of a riser (m)

Greek letters

ΔP	pressure drop
ρ_s	density of material (kg m^{-3})
Φ	shape factor

convert the bottom zone in to its compact structure. The applied field intensity causes an interparticle attraction and will turn the lower zone into small clusters, with further increase in magnetic field intensity (H) to larger cluster and finally in to a magnetically frozen bed. This change is likely to convert CFB to a batch MSB (magnetically stabilized bed). However, with the moderate field intensity this structure will be different. Magnetically aligned particles in the bottom zone with the sufficient velocity to lift them in the upper zone (core-annulus region) will put this particle in orderly structure of chains and concentration in the core as well as annulus will be homogenous. Compared to CFB reactor, the particles in a magnetically assisted CFB reactor, do not suffer as much mechanical agitation, leading to reduced particle attrition. In addition, the magnetic forces in the 'magnetically assisted circulating fluidized bed' reactor suppress the formation of gas bubbles, resulting in better interphase contacting [9].

The present investigation has been aimed in applying an axial magnetic field to a laboratory circulating fluidized bed so as to study the effect of magnetic field on pressure drop, solids holdup, at various heights along the riser.

1.1. Axial variation of solid holdup by pressure tapping technique

Many studies have come along in the literature apportioning with axial solids distribution along CFB risers [10–12]. It is most often expressed as either a plot of the axially averaged solids suspension density or voidage versus heights. This profile is experimentally resolved from the pressure distribution along the riser, realizing that the suspended solids constitute the major subscriber to the pressure drop, $\Delta P/\Delta L = \rho_P(1-\varepsilon_g)g$. This establishment neglects acceleration, gas and solid wall friction, and gas density [13].

The experimental work of Yerushalmi et al. [10] is usually conceived as the pioneering academic study of the axial solids distribution in circulating fluidized bed risers. They discoursed the densification at the riser base and suggested several advantages of operating in the fast fluidization regime. Kwauk et al. [11] manifested the coexistence of a dense phase at the bottom of the riser below a dilute phase exserting to the top of the riser, and furnished the mathematical expression for identifying the characteristic S-shaped voidage distribution that they experimentally evaluated, indicating the vague boundary between dense and dilute regions. They also circumscribed fast fluidization as the regime in which the suspension density is dilute at the top and dense at the bottom with an inflection point in between.

In the present study, the influence of magnetic field on individual and overall, pressure drop and solids holdup in the riser section of a 'magnetically assisted circulating fluidized bed' has been evaluated.

2. Experimental setup

The schematic diagram of the experimental setup is shown in Fig. 1. The experimental unit consists of a riser 0.032 m diameter column with 1.5 m height followed by cyclone. The downcomer part consists of 0.04 m pipe with a shutter arrangement for the

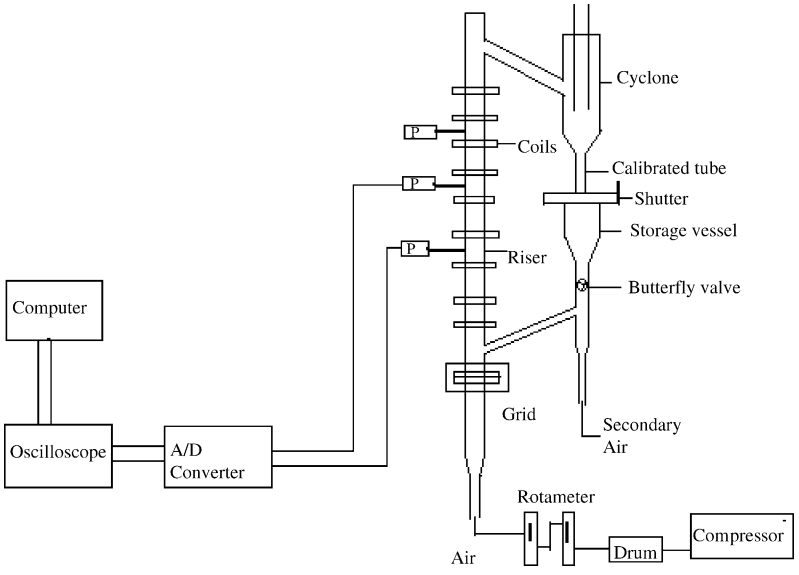

Fig. 1. Experimental setup of the 'magnetically assisted circulating fluidized bed'.

measurement of solids circulation rate. The solids were fed back to the storage vessel provided at the base with an arrangement to keep the material in the storage vessel above minimum fluidization level. The inclined pipe from the storage vessel joined to the base of the riser was provided with a butter fly valve to feed the material in the riser at desired mass flow rate. Air in the experimental range, $U_g = 4.2–5.3\ m\ s^{-1}$, has been used as fluidizing agent, whereas for the particulate phase, magnetite material with a particle size, $d_p = 425\ \mu m$ ($\Phi = 0.86$, $\rho_s = 4500\ kg\ m^{-3}$) has been used. The magnetic field was generated by eight solenoids and by adjusting the suitable distance between each solenoids, an axial uniform magnetic field can be generated. The operating mode is 'magnetization last' according to the classification of Hristov [14].

The riser is equipped with a pressure tapping at an interval of 0.3 m to detect the axial pressure profile, which helps in calculating the apparent solids holdup in that section. The solids circulation rate was calculated by adjusting certain mass flow rate of solids in the riser. When the flow was stabilized the lower butterfly valve feeding the material to the riser and shutter arrangement below the cyclone was simultaneously closed, the mass of material collected for the known time helped in getting the solids circulation flux. This was repeated for three times under the same experimental condition to obtain a mean value.

3. Results and discussion

Fig. 2(a and b) shows the axial pressure profiles of 'magnetically assisted circulating fluidized bed' riser operated at a gas velocity, $U_g = 4.5\ m\ s^{-1}$, with varying magnetic field intensity for two different solids circulation rates. The total pressure drop appears to be level off with increasing the magnetic field intensity, indicating that, the whole riser is under high-density condition. An approximately linear relationship is obtained for presence of magnetic field and absence of magnetic field having a dense bed structure at the bottom and lean bed in the upper part of the riser (Fig. 2(a and b)). The linear portion is consistent with results presented by Vander Schaaf et al. [15].

Fig. 3(a and b) shows the axial profiles of time-averaged solids holdup determined from pressure drops at a gas velocity, $U_g = 4.5\ m\ s^{-1}$ with varying field intensity for two different solids circulation rates. The local time-averaged solids holdup decreases slightly along the riser from bottom to top. For increasing solids circulation rate in presence of magnetic field, the time-averaged solids holdup increases along the riser height. In the upper part of the riser where the lean bed conditions are attained the increase in solids holdup is marginal for low intensity field ($H = 1.1825 \times 10^4\ A\ m^{-1}$) and is maximum for increasing magnetic field intensity. The interparticle attraction due to magnetic field [6–8] is the cause of such a rise in the values of pressure drop (ΔP) and solids holdup.

Figs. 4(a–c) and 5(a–c), show the axial profiles of apparent solids holdup in the riser at various solids circulation rate ($G_s = 30.1,\ 33.4,\ 37.5\ kg\ m^{-2}\ s^{-1}$) for absence of magnetic field (i.e. $H = 0\ A\ m^{-1}$) and presence of magnetic field ($H = 1.4382 \times 10^4\ A\ m^{-1}$) with varying gas velocity ($U_g = 4.2$, 4.8 and $5.3\ m\ s^{-1}$). The extremely high apparent solids holdup

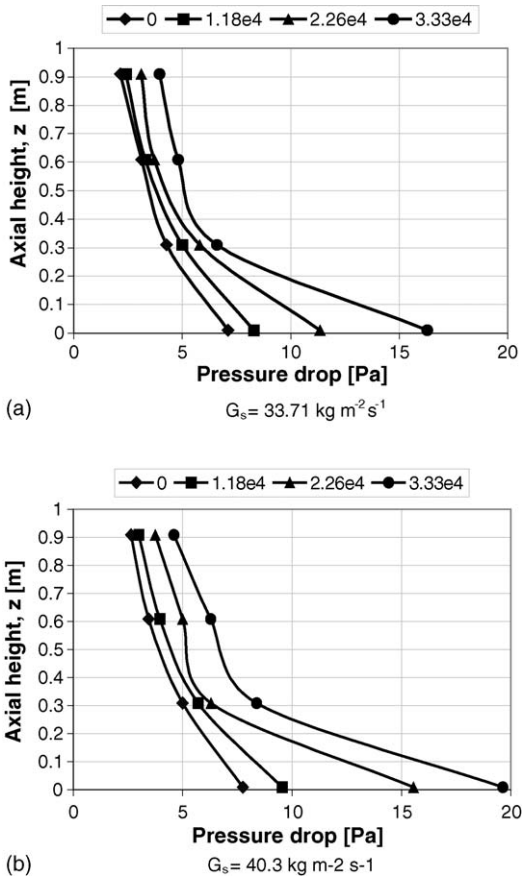

Fig. 2. Axial distribution of pressure profile at a constant gas velocity, $U_g = 4.5\ m\ s^{-1}$ (i.e. $U/U_{mf} = 10$) for two different solid circulation rate: (a) $G_s = 33.71\ kg\ m^{-2}\ s^{-1}$ and (b) $G_s = 40.3\ kg\ m^{-2}\ s^{-1}$, with varying field intensity.

recorded near the riser bottom are significantly affected by particle acceleration as well as by solids entry configuration. Beyond this region the solids holdup exponentially decreases, eventually approaching a constant value higher up the riser, or follow an S-shaped profile, with a dense phase at the bottom and a dilute region at the top. The solids holdup increases, for increasing solids circulation rates, G_s (Fig. 4(a–c)), as well as for applied magnetic field with the respective solids circulation rates (Fig. 5(a–c)) due to which, relatively dense structure covering the entire column height. While, at the same time, for the above operating condition the solids holdup decreases with increasing gas velocity (Figs. 4(a–c) and 5(a–c)). These trends are consistent with the earlier results for absence of magnetic field [16,17].

The influence of superficial gas velocity can be observed in Fig. 6(a and b), where the solids holdup between $z = 0.31$ and 0.61 m is plotted against the superficial gas velocity with solids circulation rate as the varying parameter for absence of magnetic field ($H = 0\ A\ m^{-1}$) and presence of magnetic field ($H = 1.4382 \times 10^4\ A\ m^{-1}$). At the lowest solids circulation rate, $G_s = 30.1\ kg\ m^{-2}\ s^{-1}$, the decrease in solids holdup with increasing gas velocity is relatively small. The dense phase starts to build up in the riser at low gas velocity (Fig. 6(a and b)), and a higher solids circulation rate needed to achieve high-density conditions at higher gas velocities. The variation of solids holdup

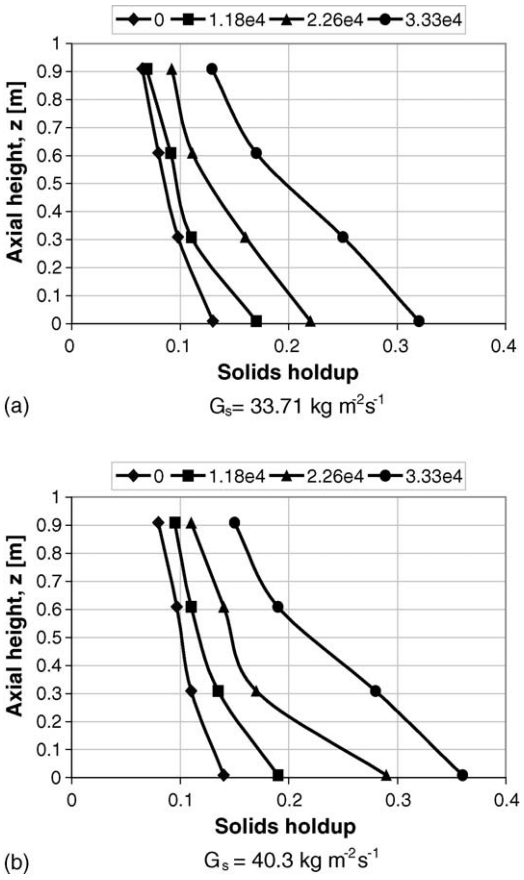

Fig. 3. Axial distribution of solid holdup at a constant gas velocity, $U_g = 4.5\,m\,s^{-1}$ (i.e. $U/U_{mf} = 10$) for two different solid circulation rate: (a) $G_s = 33.71\,kg\,m^{-2}\,s^{-1}$ and (b) $G_s = 40.3\,kg\,m^{-2}\,s^{-1}$, with varying field intensity.

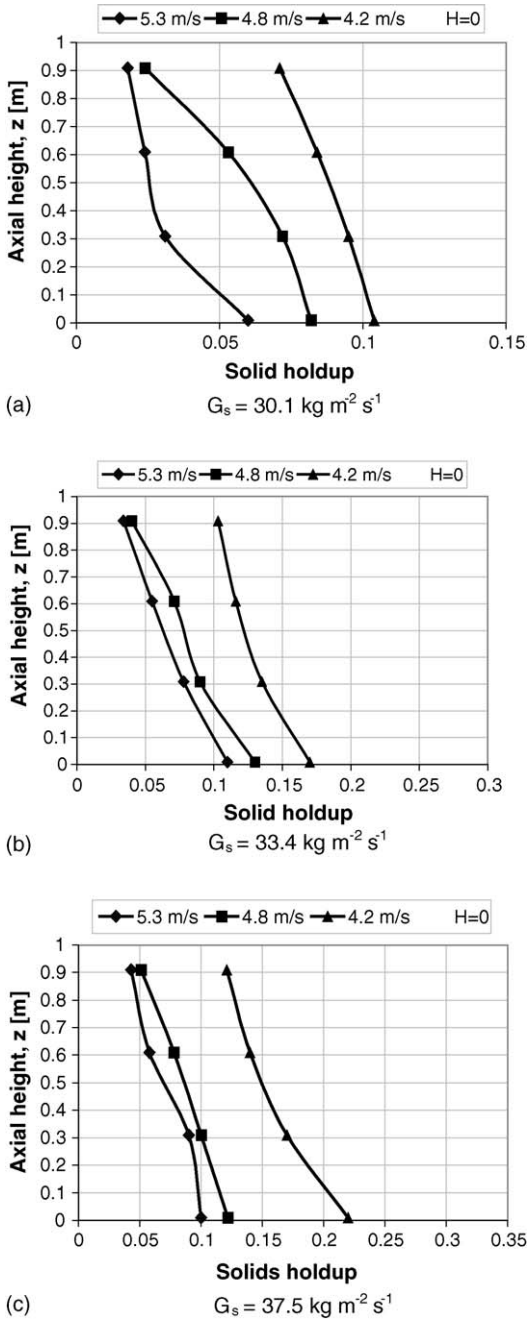

Fig. 4. Longitudinal profiles of apparent solids holdup for different solids circulation rate: (a) $G_s = 30.1\,kg\,m^{-2}\,s^{-1}$, (b) $G_s = 33.4\,kg\,m^{-2}\,s^{-1}$, (c) $G_s = 37.5\,kg\,m^{-2}\,s^{-1}$, at a magnetic field intensity, $H = 0\,A\,m^{-1}$, with varying gas velocity.

with gas velocity is again small once high-density conditions have been established.

Similarly, Fig. 7(a and b) is plotted against the superficial gas velocity between $z = 0.61$ and 0.91 m with solids circulation rate as the varying parameter for absence of magnetic field ($H = 0\,A\,m^{-1}$) and presence of magnetic field ($H = 1.4382 \times 10^4\,A\,m^{-1}$). The difference is the solids holdup is less for absence of magnetic field (Figs. 6(a) and 7(a)) compared to the presence of magnetic field (Figs. 6(b) and 7(b)), for the respective gas velocity and solids circulation rate. It is, because, with applied magnetic field the voidage decreases and the particle–particle collisions becomes more significant. Furthermore, with applied magnetic field, the formation of clusters and aggregation of solids can be considered to become more predominant.

Fig. 8 shows the plot of mean solids holdup at various heights along the riser as a function of solids circulation flux at, $U_g = 4.2\,m\,s^{-1}$ for absence of magnetic field ($H = 0\,A\,m^{-1}$) and presence of magnetic field ($H = 1.4382 \times 10^4\,A\,m^{-1}$) between $z = 0.31$–0.61 and 0.61–0.91 m. Fig. 8 shows a dense structure starts to form along the riser height when solids circulation rate increases. For low solids circulation rate, $G_s = 30.1\,kg\,m^{-2}\,s^{-1}$, the solids holdup is low and all the particles are observed to be carried upward in pneumatic transport mode [18]. As the solids circulation rate is increased, their concentration rises. Further increasing G_s leads to a point beyond which the solids can no longer be suspended individually, and the suspension collapses initiating choking and fast fluidization flow regime [19]. Besides this, when the solids circulation rate is raised further, in the dilute section above the dense zone, particles starts to move down at the wall and more solids refluxing occurs. These are all associated, with increasing solids circulation rate for absence of magnetic field (i.e. $H = 0\,A\,m^{-1}$). In order to avoid such complexicity and to increase the solids suspension density without changing the

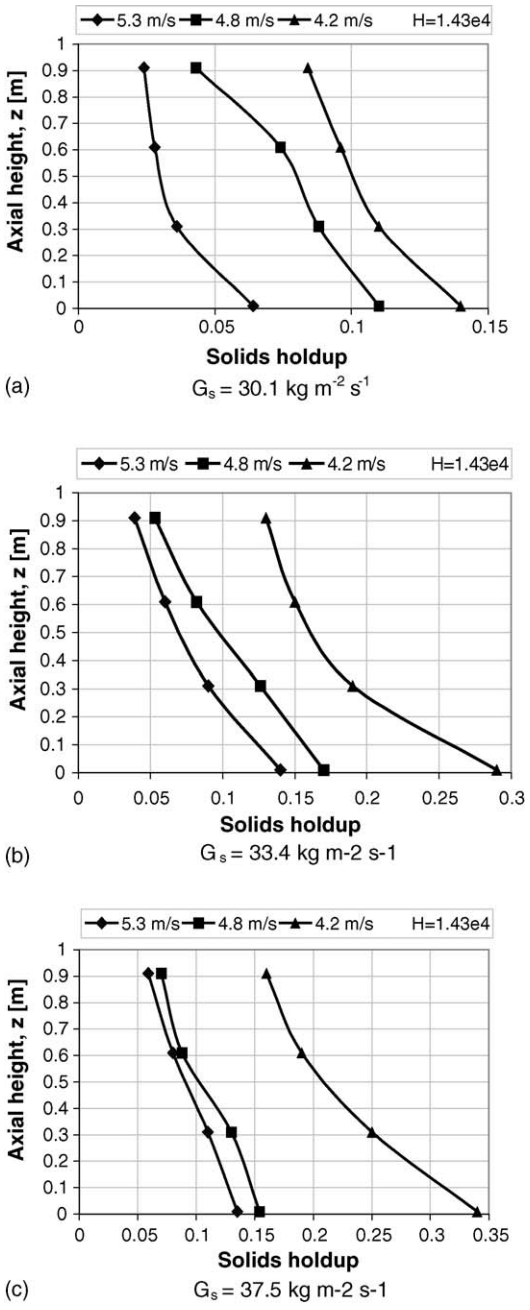

Fig. 5. Longitudinal profiles of apparent solids holdup for different solids circulation rate: (a) $G_s = 30.1\,\mathrm{kg\,m^{-2}\,s^{-1}}$, (b) $G_s = 33.4\,\mathrm{kg\,m^{-2}\,s^{-1}}$, (c) $G_s = 37.5\,\mathrm{kg\,m^{-2}\,s^{-1}}$, at a magnetic field intensity, $H = 1.43 \times 10^4\,\mathrm{A\,m^{-1}}$, with varying gas velocity.

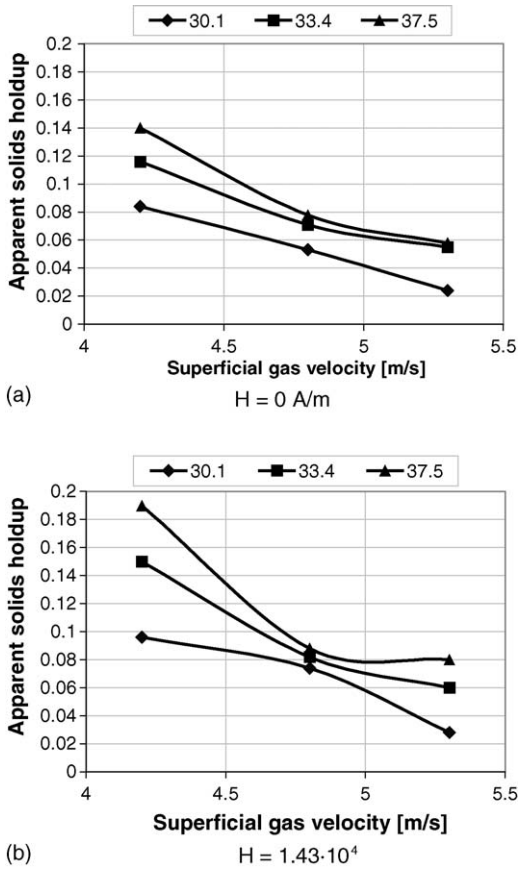

Fig. 6. Influence of superficial gas velocity on apparent solids holdup at a constant field intensity: (a) $H = 0\,\mathrm{A\,m^{-1}}$, (b) $H = 1.43 \times 10^4\,\mathrm{A\,m^{-1}}$, between $z = 0.31$ and 0.61 m for various solids circulation rates.

wide range of solids circulation fluxes, the super imposed magnetic field applied to a CFB riser.

Fig. 8 shows sharp rise in the solids holdup for presence of magnetic field compared to absence of magnetic field at the same operating conditions in a 'magnetically assisted circulating fluidized bed'. The dense region has spread to the whole section between two pressure measurement points. Since, for applied magnetic field the solids concentration increases due to interparticle attraction and they formed a cluster, due to which the dense suspension encroaches further and further up the riser and this dense region exhibits relatively homogeneous flow structure as compared to absence of magnetic field (Figs. 3(b) and 8). The solids refluxing usually observed near the wall of a dilute CFB risers (for absence of magnetic field), no longer exists; instead the whole suspension appears to be relatively homogeneous with moderate upward and downward velocity fluctuations.

It has merited attention, that the solids holdup is level off by the application of magnetic field along the whole riser section, without increasing the solids circulation rate. The achievable difference for presence of magnetic field and absence of magnetic field is shown in Fig. 8. Since, the dense region expands for the applied magnetic field the intersection points differ for each height, i.e. different levels in the riser attains high-density condition in presence of magnetic field for the given superficial gas velocity.

For the dilute section between $z = 0.31$–0.61 and 0.61–0.91 m, seen in Figs. 8, 6(b), 7(b), and 3(b), it is predictable, that the magnetic field has a significant influence on fluidization phenomenon along the whole riser section and appears that, for the applied magnetic field the solids holdup begins to increase. This most likely indicates the starts of a 'transition' towards much 'denser' suspension.

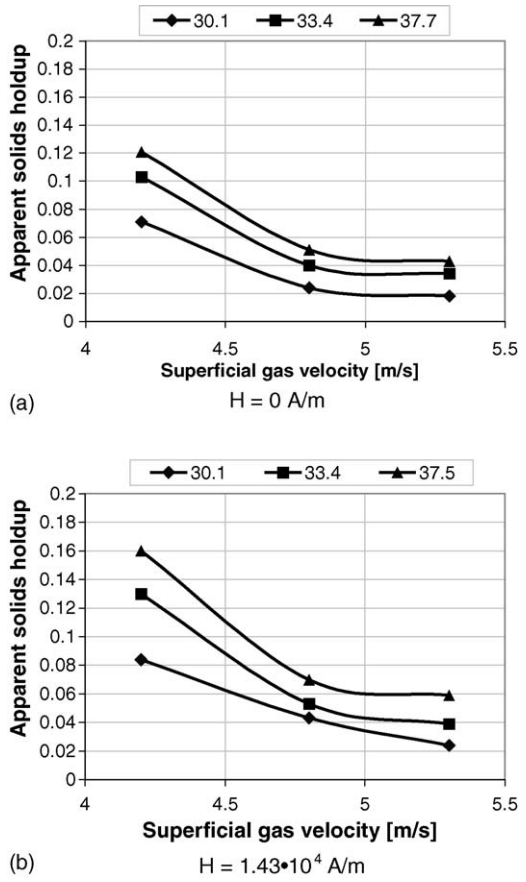

Fig. 7. Influence of superficial gas velocity on apparent solids holdup at a constant field intensity: (a) $H = 0\ \mathrm{A\,m^{-1}}$, (b) $H = 1.43 \times 10^4\ \mathrm{A\,m^{-1}}$, between $z = 0.61$ and 0.91 m for various solids circulation rates.

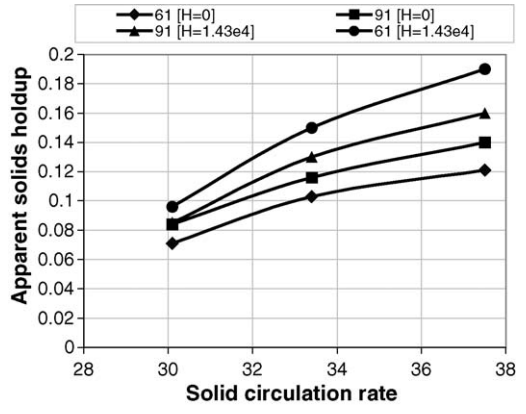

Fig. 8. Apparent solids holdup as a function of solids circulation rate between $z = 0.31$–0.61 and 0.61–0.91 m, at a constant gas velocity, $U_g = 4.2\ \mathrm{m\,s^{-1}}$ for two different field intensities, $H = 0$ and $1.43 \times 10^4\ \mathrm{A\,m^{-1}}$.

4. Conclusion

The pressure drop and solids holdup increases along the riser height, with increasing magnetic field intensity. They were found to correspond to gas–solids turbulent interaction due to magnetic field intensity and solids circulation rate.

The extremely high apparent solids holdup recorded near the riser bottom and beyond this region the solids holdup exponentially decreases, or follows an S-shaped profile, with a dense phase at the bottom and a dilute region at the top. For varying superficial gas velocity and solids circulation rate, the increase of solids holdup for absence of magnetic field is less compared to presence of magnetic field.

Since, with the applied magnetic field the voidage decreases and the particle–particle collisions become more significant. Furthermore, with increasing the magnetic field intensity, the formation of clusters or aggregation of solids can be considered to become more predominant, due to which the dense suspension encroaches further and further up the riser. This dense region exhibits a relatively homogeneous flow structure as compared to absence of magnetic field (Figs. 3(b) and 8).

From the 'magnetically assisted circulating fluidized bed', it is predictable, that the magnetic field has a significant influence on fluidization phenomenon along the whole riser, especially for the dilute section. It appears that, for applied magnetic field with the respective solids circulation fluxes, the solids holdup begins to increase. This most likely indicates the starts of a 'transition' towards much 'denser' suspension.

References

[1] A.A. Avidan, Fluid catalytic cracking, in: J.R. Grace, A.A. Avidan, T.M. Knowlton (Eds.), Circulating Fluidized Beds, Blackie Academic and Professional, London, 1997, p. 119.
[2] A.M. Squires, M. Kwauk, A.A. Avidan, Fluid beds: at last, challenging two entrenched practices, Science 230 (1985) 1329.
[3] B. Sun, W.J. Koves, Application of a numerical hydrodynamic model in FCC design, Particle Technol. Forum, vol. 2, AIChE, Miami Beach, FL, 1998, p. 469.
[4] Y. Jin, J.X. Zhu, Z.Q. Yu, Novel configurations and variants, in: J.R. Grace, A.A. Avidan, T.M. Knowlton (Eds.), Circulating Fluidized Beds, Blackie Academic and Professional, London, 1997, p. 525.
[5] A. Therdthianwong, D. Gidaspow, Hydrodynamics SO_2 sorption in a CFB loop, circulating fluidized bed technology, vol. IV, in: A.A. Avidan (Ed.), Proc. AIChE Int. Conf. On Circulating Fluidized Beds, New York, 1994, p. 551.
[6] R.E. Rosenweig, J.H. Siegel, W.K. Lee, T. Mikus, Magnetically stabilized fluidized solids, AIChE Symp. Ser. 77 (1981) 8.
[7] I.P. Penchev, J.Y. Hristov, Behaviour of fluidized beds of ferromagnetic particles in an axial magnetic field, Powder Technol. 61 (1990) 103.
[8] R.L. Sonolikar, Magneto fluidized beds, in: A. Mujumdar (Ed.), Transport in Fluidized Particle Systems, Elsevier, New York, 1989, p. 359.
[9] J.C. Pirkle, P.A. Ruziska, L.J. Shulik, Circulating magnetically stabilized bed reactors, Chem. Eng. Commun. 67 (1988) 89.
[10] J. Yerushalmi, D.H. Turner, A.M. Sqires, The fast fluidized bed, Ind. Eng. Chem. Process Des. Dev. 15 (1976) 47.
[11] M. Kwauk, W. Ningde, L. Youchu, C. Bingyu, S. Zhiyan, Fast fluidization at ICM, in: P. Basu (Ed.), Circulating Fluidized Bed Technology I, 1986, p. 33.
[12] H. Ohara, H. Ji, K. Kuramoto, A. Tsutsumi, K. Yoshida, T. Hirama, Chaotic characteristic of local voidage fluctuation in a circulating fluidized bed, Can. J. Chem. Eng. 77 (1999) 247.
[13] M. Louge, H. Chang, Pressure and voidage gradients in vertical gas–solid risers, Powder Technol. 60 (1990) 197.
[14] J.Y. Hristov, Magnetic field assisted fluidization—a unified approach. Part 2. Solids batch gas-fluidized beds: versions and rheology, Rev. Chem. Eng. 19 (2003) 1.

[15] J. Van der Schaaf, J.C. Schouten, F. Johnsson, C.M. van den Bleek, Non-intrusive determination of bubble and slug length scales in fluidized beds by decomposition of the power spectral density of pressure time series, Int. J. Multiphase Flow 28 (2002) 865.
[16] Y. Li, M. Kwauk, The dynamics of fast fluidization, in: J.R. Grace, J.M. Matsen (Eds.), Fluidization, Plenum Press, New York, 1980, p. 537.
[17] U. Arena, A. Cammarota, L. Pistone, High velocity fluidization behavior of solids in a laboratory scale circulating fluidized bed, in: P. Basu (Ed.), Circulating Fluidized Bed Technology I, 1986, p. 119.
[18] H.T. Bi, J.R. Grace, Flow patterns in high-velocity fluidized beds and pneumatic conveying, Can. J. Chem. Eng. 77 (1999) 223.
[19] H.T. Bi, J.R. Grace, J.X. Zhu, On type of choking in pneumatic system, Int. J. Multiphase Flow 19 (1993) 1077.